

Argyrios Chronopoulos,¹ Sumon Roy,¹ Ekaterina Beglova,¹ Keith Mansfield,² Lynn Wachtman,² and Sayon Roy¹



Hyperhexosemia-Induced Retinal Vascular Pathology in a Novel Primate Model of Diabetic Retinopathy

Diabetes 2015;64:2603–2608 | DOI: 10.2337/db14-0866

The paucity of animal models exhibiting full pathology of diabetic retinopathy (DR) has impeded understanding of the pathogenesis of DR and the development of therapeutic interventions. Here, we investigated whether hyperhexosemic marmosets (*Callithrix jacchus*) develop characteristic retinal vascular lesions including macular edema (ME), a leading cause of vision loss in DR. Marmosets maintained on 30% galactose (gal)-rich diet for 2 years were monitored for retinal vascular permeability, development of ME, and morphological characteristics including acellular capillaries (AC) and pericyte loss (PL), vessel tortuosity, and capillary basement membrane (BM) thickness. Excess vascular permeability, increased number of AC and PL, vascular BM thickening, and increased vessel tortuosity were observed in the retinas of gal-fed marmosets. Optical coherence tomography (OCT) images revealed significant thickening of the retinal foveal and the juxtafoveal area, and histological analysis showed incipient microaneurysms in retinas of gal-fed marmosets. Findings from this study indicate that hyperhexosemia can trigger retinal vascular changes similar to those seen in human DR including ME and microaneurysms. The striking similarities between the marmoset retina and the human retina, and the exceptionally small size of the monkey, offer significant advantages to this primate model of DR.

Diabetic retinopathy (DR) and particularly diabetic macular edema (DME) are leading causes of blindness (1–3). Currently, the lack of an efficient animal model of DR has been a major drawback in understanding the pathogenesis of DR and developing novel treatment strategies. The

common marmoset (*Callithrix jacchus*) is a new world primate, which is an unusually small primate that is phylogenetically close to humans, survives well in captivity, weighs ~400 g, and has relatively large eyes that are half the size of the human eye with similar retinal anatomy including the presence of macula. The small size of the primate permits convenient handling and low maintenance costs. Furthermore, the successful creation of transgenic marmosets offers unique opportunities in the way we could study DR (4). Although marmosets have been used as animal models of various diseases (5–7), to date the feasibility of using the marmoset as a model of DR has not been studied (8–10). Here, we have investigated whether hyperglycemic marmosets develop retinal vascular lesions and evaluated its validity as a model of DR.

RESEARCH DESIGN AND METHODS

Marmoset Handling

Four marmosets were kept on a 30% galactose (gal)-rich diet (LabDiet, Richmond, IN) in an animal colony at the New England Primate Research Center, Harvard Medical School, for a period of 2.5 years under an experimental protocol approved by Harvard Medical School's Standing Committee on Animals as well as the tenets of the Association for Research in Vision and Ophthalmology Statement for the Use of Animals in Ophthalmic and Vision Research. Two marmosets were maintained in parallel as normal controls. HbA_{1c} levels were measured every 3 months using a kit (Glyc-Affin; Pierce, Rockford, IL), and fasting blood glucose levels were assessed routinely using a glucometer (OneTouch Ultra; LifeScan, Inc., Milpitas, CA).

¹Departments of Medicine and Ophthalmology, Boston University School of Medicine, Boston, MA

²New England Primate Research Center, Harvard Medical School, Southborough, MA
Corresponding author: Sayon Roy, sayon@bu.edu.

Received 30 May 2014 and accepted 19 February 2015.

A.C. and S.R. contributed equally to this work.

© 2015 by the American Diabetes Association. Readers may use this article as long as the work is properly cited, the use is educational and not for profit, and the work is not altered.

Retinal Trypsin Digest and Assessment of Endothelial Cell-to-Pericyte Ratio, Acellular Capillaries and Pericyte Loss, and Vessel Tortuosity

The retinal trypsin digest (RTD) method was performed as previously described (11). Briefly, whole retinas were dissected, fixed in 10% formalin, and placed in 0.15 mol/L glycine buffer overnight. The following day, retinas were immersed in 3% trypsin (BD Biosciences, San Jose, CA) at 37°C for ~3 h to allow for glial digestion. The nonvascular mass was gently removed with a brush (Ted Pella, Redding, CA) and the isolated retinal vascular network mounted onto silane-coated slides and stained with periodic acid Schiff and hematoxylin-eosin. At least 10 random areas were photographed using the Nikon microscope attached to the Nikon F1 digital camera. The images were assessed for endothelial cell (EC)-to-pericyte ratio, number of acellular capillaries (AC) and pericyte loss (PL), and microaneurysms. Vessel tortuosity was assessed by the distance factor formula based on arc-to-chord ratio (12,13).

Electron Microscopy

The retinas were fixed in 2.5% glutaraldehyde in 0.1 mol/L cacodylate buffer and dehydrated using osmium tetroxide, ethanol, and propylene oxide (EMS, Hatfield, PA). The tissues were then embedded in an Epon-Araldite. Sectioning was performed at 60–70 nm using a microtome (Ultratome Nova; LKB, Bromma, Sweden), and sections were placed on a copper grid, stained with 4% uranyl acetate in methanol, and viewed under a transmission electron microscope (Philips Electron Optics, Eindhoven, the Netherlands). At least 10 random images of retinal capillaries were photographed and examined according to the orthogonal intercept method for basement membrane (BM) thickness (14).

Measurement of Retinal Capillary BM Thickness

BM thickness was determined as previously described (14). Briefly, a 20-spoke radial grid was superimposed over a retinal capillary transverse section, and BM thickness was noted at each point that a spoke intersected the BM. The width of the two thinnest BM portions surrounding each vessel was also measured and entered into the overall assessment excluding overlapped areas of BM from ECs and pericytes.

Assessment of Retinal Vascular Permeability

For assessment of retinal vascular leakage, marmosets were anesthetized by intramuscular injection of ketamine (25 mg/kg) followed by 0.5 mL of 5% fluorescein isothiocyanate (FITC)-BSA through the saphenous vein. The marmosets were killed with an overdose of intravenous pentobarbital and their eyes enucleated. Retinas were imaged under fluorescence microscope (Diaphot; Nikon, Tokyo, Japan) attached to a Nikon F1 digital camera (Nikon Instruments, Melville, NY).

OCT Imaging

Retinal imaging was performed at 3- to 4-month intervals with a high-speed spectral domain OCT (SD-OCT; Optovue, Fremont, CA), which was slightly modified to adjust

for the shorter visual axis of the marmoset eye (~12 mm). After anesthesia, the pupils were dilated with one drop of AK-Dilate 2.5% phenylephrine hydrochloride (Akorn, Inc., Buffalo Grove, IL) and one drop of 1% tropicamide (Bausch & Lomb, Tampa, FL).

Western Blot Analysis

Total protein was isolated from the marmoset retinas and Western Blot analysis was performed as previously described (15). Briefly, retinas were placed in lysis buffer (25 mmol/L Tris, 1 mmol/L EDTA, and 0.1% Triton X-100) and homogenized, and total protein was extracted. Equal amounts of protein was electrophoresed, and the gel was transferred to nitrocellulose membranes (Bio-Rad, Hercules, CA), blocked with 5% nonfat dry milk, and exposed to rabbit anti-human fibronectin (FN) antibody overnight (1:1000) (Millipore, Billerica, MA). After washes, the membrane was incubated with goat anti-rabbit secondary antibody (1:3,000; Cell Signaling Technology, Danvers, MA) for 1 h and exposed to Immun-Star Chemiluminescent Protein Detection System (Bio-Rad), and signals were captured on an X-ray film (Fujifilm, Tokyo, Japan). Equal protein loading was confirmed by β -actin densitometric analysis.

Statistical Analysis

Data were analyzed for statistical significance using a two-tailed Student *t* test to compare the specific differences between groups. Data are presented as mean \pm SD. In all analyses, statistical significance was determined when $P < 0.05$.

RESULTS

Marmoset Eye and Its Structural Characteristics of the Retinal Capillary Network

The marmoset is an unusually small primate weighing 387 ± 12 g, and the adult marmoset eyeball is ~13 mm in diameter (Fig. 1A and B). The macula is located 2.5 disc diameters from the optic disc with a prominent foveal avascular zone (Fig. 1C and D). Additionally, a prominent depression in the central area of the foveal pit and the retinal arteriolar and venular arcade around the macula as well as the vessel tortuosity indices resembled those of the human retina. Furthermore, the 1:0.9 ratio of ECs to pericytes in the marmoset retinal capillaries is similar to that of the human retina.

Blood Glucose and HbA_{1c} Level

The fasting blood glucose measurements and the HbA_{1c} levels showed significant increase in the gal-fed marmosets (215 ± 64 mg/dL, $8.7 \pm 1.8\%$) compared with those of the control marmosets (98 ± 18 mg/dL, $5.03 \pm 1.9\%$).

Histological Assessment of Microaneurysms, AC, and PL in the Marmoset Retinal Capillaries

In two of the four gal-fed marmosets, small vascular outpouchings were observed indicating incipient microaneurysms (Fig. 1E). The number of AC and PL was significantly increased in gal-fed marmosets compared with those of control marmosets ($221 \pm 35\%$ of control,

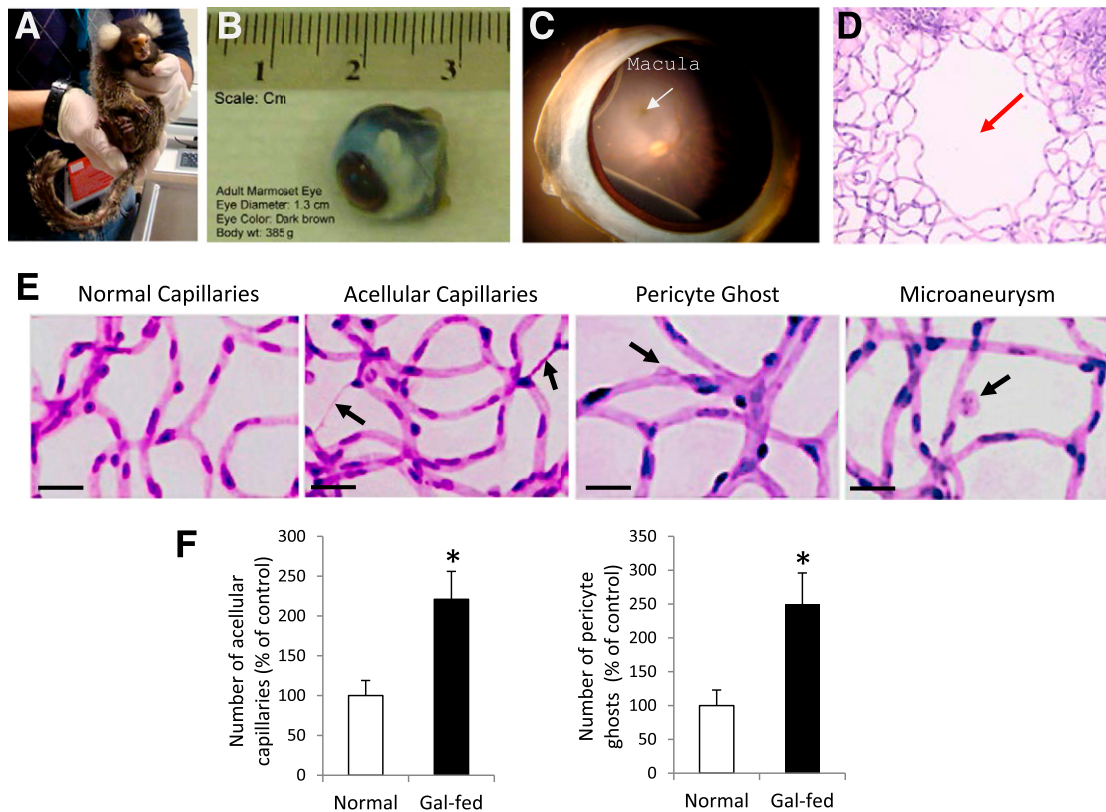


Figure 1—Marmoset eye, macula, and retinal capillary network surrounding macular area and acellular capillaries, pericyte loss, and microaneurysms in gal-fed marmoset. *A*: Marmoset is an unusually small primate. *B*: An adult marmoset eyeball is ~13 mm in diameter. *C*: Marmoset macula (white arrow) is present at an ~2.5 disc diameter distance from the optic disc. *D*: A prominent foveal avascular zone is located in the macula (red arrow). Note that the relative size and location of macula with respect to the optic disc in the marmoset retina are strikingly similar to those of the human macula. *E*: Effect of hyperhexosemia on retinal vascular lesions characteristic of DR. Representative images of retinal capillary network show increased number of acellular capillaries and pericyte loss in the retinas of gal-fed marmosets compared with those of control marmosets. Incipient microaneurysms were detected in the gal-fed marmosets. Magnification bar: 20 $\mu\text{mol/L}$. *F*: Graphical illustrations showing significant increase in the number of acellular capillaries (left) and pericyte ghosts (right) in the retinas of gal-fed marmosets compared with those of control marmosets. * $P < 0.05$.

$P < 0.01$, and $250 \pm 46\%$ of control, $P < 0.02$, respectively) (Fig. 1*F*).

Vascular BM Thickening and Overexpression of FN in the Marmoset Retina

Retinal vascular BM thickening was significantly increased in the gal-fed marmosets compared with those of control marmosets (147 ± 34 nm vs. 244 ± 30 nm, $P < 0.02$) (Fig. 2). Western blot analysis indicated significant overexpression of FN in the retinas of gal-fed marmosets compared with those of control marmosets ($169 \pm 14\%$ of normal, $P < 0.05$).

Assessment of Vascular Permeability in the Marmoset Retina

In the retinal vessels of control marmosets, limited fluorescence intensity was visible, whereas in the retinal vessels of the gal-fed marmosets, areas of extravasation were evident, indicative of increased vascular permeability. The presence of a number of retinal capillaries exhibiting vascular permeability in the gal-fed marmosets (Fig. 3) clearly indicated compromised blood retinal barrier.

Assessment of Retinal Thickness and Macular Edema Using OCT

The OCT scans of normal marmosets provided baseline values for the normal macular thickness, which was 156 ± 19.7 μm in the fovea and 248 ± 11.4 μm in the juxtafoveal area (Fig. 4*A–C*) with 232, 228, 242, and 237 μm in the temporal, nasal, superior, and inferior orientations, respectively.

Of the four gal-fed marmosets, one showed signs of cystoid retinal edema (Fig. 4*F*) with an overall foveal thickness at 210 μm in the optical density (OD) and 206 μm in the oculus sinister (OS). A juxtafoveal increase with 292, 280, 288, and 281 μm temporally, nasally, superiorly, and inferiorly, respectively, with indications of intraretinal fluid accumulation was also noted. Interestingly, the discontinuation of the photoreceptor layer, indicative of intraretinal fluid accumulation representing early stages of edematous retina (Fig. 4*D*), and the choroidal effusion in the OD (Fig. 4*D* and *E*) were increasingly evident toward the end of the study (Fig. 4*A–C* and *E*). The foveal thickness in the OS of the same marmoset was 209 μm with a juxtafoveal thickness of 285, 291, 292,

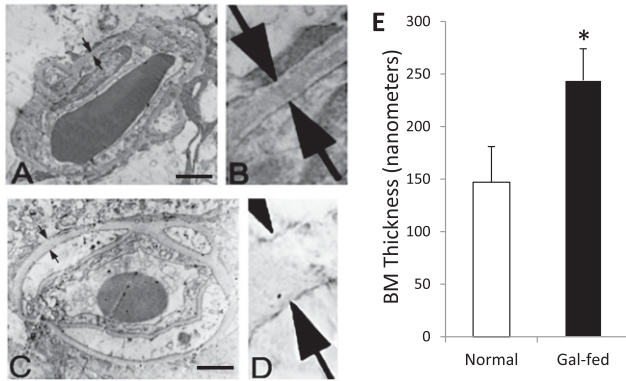


Figure 2—Capillary BM thickness in retinas of marmoset. BM thickness (arrows) in transverse sections of a retinal capillary from normal marmoset (A). B: Corresponding enlarged view. C: Gal-fed marmoset. D: Corresponding enlarged view. Magnification bar: 1 $\mu\text{mol/L}$. E: Graphical illustration of capillary BM thickness in retinas of normal and gal-fed marmoset. * $P < 0.02$.

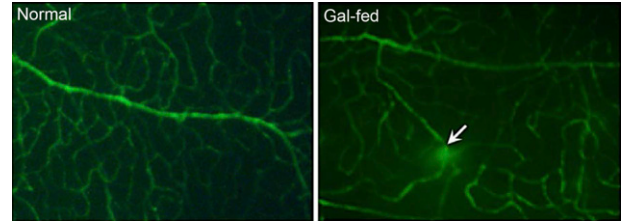


Figure 3—Retinal vascular permeability in gal-fed marmoset. Representative areas showing FITC fluorescence in vessels of whole-mount retinas. Areas of intense FITC leakage from extravasation were observed in the retinas of gal-fed marmosets compared with those of control normoglycemic marmosets. In the gal-fed marmoset retinas, some vessels showed vascular leakage at specific points of the vessel (arrow).

and 277 μm (temporally, nasally, superiorly, and inferiorly). Furthermore, the alterations at the retinal pigment epithelium (RPE) level over a period of 3–4 months suggest fluid accumulation, and an intraretinal alteration resembling edema with possible tractional components was also observed (Fig. 4D and F).

The second marmoset exhibited increased foveal thickness in the OD (203 μm) but relatively less in the OS (178 μm). The juxtafoveal orientations revealed 256, 265, 258, and 269 μm of the OD and 260, 261, 268, and 256 μm of the OS (temporal, nasal, superior, and inferior, respectively). The foveal thickness in the OD of the third marmoset reached 238 μm . Owing to technical difficulties, only the temporal and nasal orientations were recorded in the OD (273 and 288 μm , respectively). The

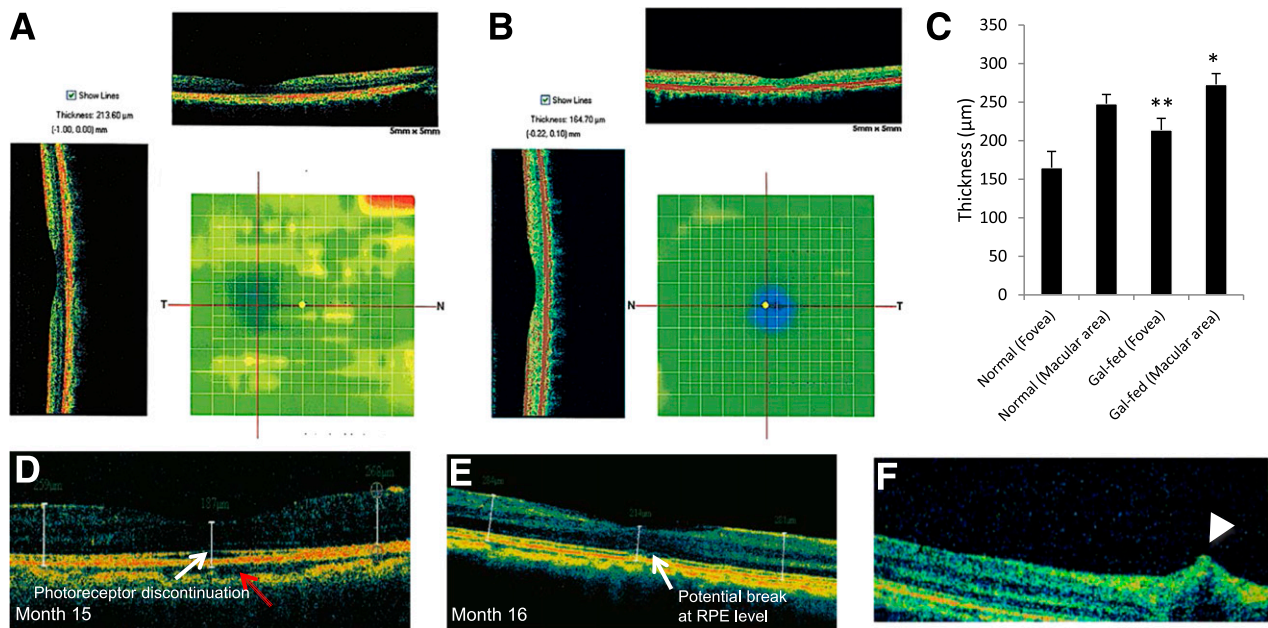


Figure 4—Representative retinal OCT scans of a gal-fed marmoset and a normal marmoset and pathological changes in the retinas of gal-fed marmosets. Significant thickening of the foveal and the juxtafoveal area, indicative of intraretinal fluid accumulation, was observed in retinas of gal-fed marmosets. Color heat images show increased foveal thickness in retinas of a gal-fed marmoset (A) compared with the foveal thickness of a normal marmoset (B). C: Graphical illustration showing macular and foveal thickness in retinas of control and galactose-fed marmosets. * $P < 0.03$, ** $P < 0.02$. D–F: Representative images of the macular area showing alterations in RPE, photoreceptor layer, and an incipient cystoid retinal edema in gal-fed marmosets. D: Fluid accumulation in the choroid (red arrow) and discontinuation at the photoreceptor layer (white arrow) representing early stages of edematous retina were observed in a gal-fed marmoset. E: Retinal thickening was accompanied by changes in RPE and retinal photoreceptor layer starting at the fifteenth month of galactose feeding. F: An OCT scan of the central retina showing a hyporeflective space just above the RPE level indicative of intraretinal fluid accumulation (arrowhead).

temporal, nasal, superior, and inferior orientation revealed 282, 281, 295, and 281 μm of the OD and 237, 248, 248, and 241 μm of the OS, respectively. The fourth gal-fed marmoset exhibited similar macular thickening.

DISCUSSION

In this study, we investigated the feasibility of the gal-fed marmoset as a primate model of DR. The presence of a macula with a foveal avascular zone, the characteristic vascular pattern and tortuosity, and the ratio of ECs to pericytes resemble the human anatomy. Additionally, the increased retinal capillary BM thickening, overexpression of FN, increased number of AC and PL, presence of microaneurysms, increased vascular permeability, and development of macular edema in the gal-fed marmosets resemble characteristics of human DR.

Several groups have attempted to develop primate models of DR using large primates and have observed some signs of DR (16,17). However, these models require ~15 years of diabetes before exhibiting retinal vasculopathy, making them impractical and unsuitable for research purposes (18). The slow progression of DR, the long gestational periods, and the low birth rates in these primates also pose formidable hurdles in developing them as primate models of DR (18).

An intriguing aspect in animal models of diabetes involving different species is the variable duration of diabetes or hyperglycemia needed to induce the development of retinal vascular lesions (19–21). This may be attributable to the longevity of the animal and its BMI (22). Studies indicate that diabetic animals with shorter life span or smaller BMI tend to develop retinal vascular lesions within a relatively short period after induction of diabetes (18). It is currently unknown how long marmosets would take to develop retinal vascular lesions under the diabetic condition. It is noteworthy that the marmoset eyeball is relatively large with respect to its body size. Furthermore, in comparison with the large primates, maintenance cost of marmosets and risk in handling are significantly lower. Additionally, studies have documented similarity in gene expression changes related to DR, such as retinal FN overexpression present in gal-fed rats, diabetic rats, and diabetic humans (15,23,24), lending credence to the validity of the marmoset model of DR. However, further studies are warranted for establishing these findings in a diabetic marmoset model.

In conclusion, the gal-fed marmoset not only exhibits histological and biochemical changes associated with DR but also shows that hyperhexosemia alone can promote the development of macular edema. The availability of the marmoset genome sequence (GenBank Assembly ID GCA_000004665.1) offers a significant advantage in designing gene modulatory strategies for the treatment of DME as well as other macular complications. Moreover, the ability to monitor retinal changes through OCT would permit longitudinal studies at a significantly low cost. Taken together, the gal-fed marmoset offers a unique

opportunity to study the pathogenesis of DR in a setting that is a significant step closer to human DR.

Funding. The research was supported by JDRF (to Sa.R.) and in part by a departmental grant from the Massachusetts Lions Eye Research Fund (to Sa.R.).

Duality of Interest. No potential conflicts of interest related to this article were reported.

Author Contributions. A.C. conducted experiments, performed protein analysis and OCT imaging, contributed to manuscript writing, and reviewed the manuscript. Su.R. assisted with the animal studies, conducted studies related to protein analysis and OCT imaging, contributed to manuscript writing, and reviewed the manuscript. E.B. conducted studies related to protein analysis and permeability assay. K.M. provided housing facilities for the marmosets, provided veterinarian care, procured tissue samples, and reviewed the manuscript. L.W. provided veterinarian care, procured tissue samples, and reviewed the manuscript. Sa.R. planned and supervised the studies, analyzed data, and wrote the manuscript. Sa.R. is the guarantor of this work and, as such, had full access to all the data in the study and takes responsibility for the integrity of the data and the accuracy of the data analysis.

References

1. Sloan FA, Bethel MA, Ruiz D Jr, Shea AM, Feinglos MN. The growing burden of diabetes mellitus in the US elderly population. *Arch Intern Med* 2008;168:192–199; discussion 199
2. Guariguata L, Whiting D, Weil C, Unwin N. The International Diabetes Federation diabetes atlas methodology for estimating global and national prevalence of diabetes in adults. *Diabetes Res Clin Pract* 2011;94:322–332
3. Klein R, Klein BE, Moss SE, Davis MD, DeMets DL. The Wisconsin epidemiologic study of diabetic retinopathy. IV. Diabetic macular edema. *Ophthalmology* 1984;91:1464–1474
4. Sasaki E, Suemizu H, Shimada A, et al. Generation of transgenic non-human primates with germline transmission. *Nature* 2009;459:523–527
5. Eslamboli A. Marmoset monkey models of Parkinson's disease: which model, when and why? *Brain Res Bull* 2005;68:140–149
6. Genain CP, Hauser SL. Creation of a model for multiple sclerosis in *Callithrix jacchus* marmosets. *J Mol Med (Berl)* 1997;75:187–197
7. Virley D, Hadingham SJ, Roberts JC, et al. A new primate model of focal stroke: endothelin-1-induced middle cerebral artery occlusion and reperfusion in the common marmoset. *J Cereb Blood Flow Metab* 2004;24:24–41
8. Dufrane D, van Steenberghe M, Guiot Y, Goebbels RM, Saliez A, Gianello P. Streptozotocin-induced diabetes in large animals (pigs/primates): role of GLUT2 transporter and beta-cell plasticity. *Transplantation* 2006;81:36–45
9. Jonasson O, Jones CW, Bauman A, John E, Manaligod J, Tso MO. The pathophysiology of experimental insulin-deficient diabetes in the monkey. Implications for pancreatic transplantation. *Ann Surg* 1985;201:27–39
10. White JA, Bolstridge MC, Downing HJ, Helm EH, Klomfass HJ. Diabetogenic drugs in the vervet monkey. *S Afr Med J* 1974;48:273–276
11. Roy S, Tonkiss J, Roy S. Aging increases retinal vascular lesions characteristic of early diabetic retinopathy. *Biogerontology* 2010;11:447–455
12. Benitez-Aguirre P, Craig ME, Sasongko MB, et al. Retinal vascular geometry predicts incident retinopathy in young people with type 1 diabetes: a prospective cohort study from adolescence. *Diabetes Care* 2011;34:1622–1627
13. Kalitzeos AA, Lip GY, Heitmar R. Retinal vessel tortuosity measures and their applications. *Exp Eye Res* 2013;106:40–46
14. Siperstein MD, Unger RH, Madison LL. Studies of muscle capillary basement membranes in normal subjects, diabetic, and prediabetic patients. *J Clin Invest* 1968;47:1973–1999
15. Cherian S, Roy S, Pinheiro A, Roy S. Tight glycemic control regulates fibronectin expression and basement membrane thickening in retinal and glomerular capillaries of diabetic rats. *Invest Ophthalmol Vis Sci* 2009;50:943–949

16. Tso MO, Kurosawa A, Benhamou E, Bauman A, Jeffrey J, Jonasson O. Microangiopathic retinopathy in experimental diabetic monkeys. *Trans Am Ophthalmol Soc* 1988;86:389–421
17. Büchi ER, Kurosawa A, Tso MO. Retinopathy in diabetic hypertensive monkeys: a pathologic study. *Graefes Arch Clin Exp Ophthalmol* 1996;234:388–398
18. Robinson R, Barathi VA, Chaurasia SS, Wong TY, Kern TS. Update on animal models of diabetic retinopathy: from molecular approaches to mice and higher mammals. *Dis Model Mech* 2012;5:444–456
19. Engerman R. Diabetes-like preproliferative retinal changes in galactose-fed dogs. *Arch Ophthalmol* 1993;111:584–585
20. Engerman RL, Kern TS. Experimental galactosemia produces diabetic-like retinopathy. *Diabetes* 1984;33:97–100
21. Wallow IH, Engerman RL. Permeability and patency of retinal blood vessels in experimental diabetes. *Invest Ophthalmol Vis Sci* 1977;16:447–461
22. Kobayashi T, Kubo E, Takahashi Y, Kasahara T, Yonezawa H, Akagi Y. Retinal vessel changes in galactose-fed dogs. *Arch Ophthalmol* 1998;116:785–789
23. Roy S, Cagliero E, Lorenzi M. Fibronectin overexpression in retinal microvessels of patients with diabetes. *Invest Ophthalmol Vis Sci* 1996;37:258–266
24. Roy S, Lorenzi M. Early biosynthetic changes in the diabetic-like retinopathy of galactose-fed rats. *Diabetologia* 1996;39:735–738